Proceedings of the 17th World Congress
The International Federation of Automatic Control
Seoul, Korea, July 6-11, 2008

Modular Design and Simulation Study of Biomimetic Snake Robots

Shang-Wei Yeh and Feng-Li Lian

Electrical Engineering Department, National Taiwan University, Taipei, Taiwan,
(e-mail: r95921067@ntu.edu.tw,and fengli@ntu.edu.tw)

Abstract: The paper discusses the design of a biomimetic snake module. The focus is on the simulation analysis of such universal mechanical modules. Based on surveyed materials from biological and robotic resources, we have successfully design two types of snake robots: wheeled and non-wheeled. Both are analyzed and tested numerically in the mechanism software: Working Model 3D. Several scenarios are tested and extensive analyses are performed.

1. INTRODUCTION

In nature, there are plenty kinds of creatures. All of them, especially snakes, develop their own features to adapt different environments. Although snakes have no limbs, they can, however, move, crawl or swim in desert, trees or water. The mobility of a new type vehicle can be realized by understanding the key principle of locomotion performed by snakes.

Taiwan is in the area that earthquakes happen frequently. Each time when earthquakes happen, buildings are destroyed and it is hard to explore and rescue the survivors. Hence, a snake-like rescue robot, which has a high degrees of freedom and excellent terrain adaptability, can be used for exploration, rescue, and even common transportation.

Real snakes develop a lot of locomotion postures to adapt to different terrains and environments. In general, there are four common modes of snake locomotion. (1) Serpentine: This is the most common locomotion mode. Snakes swing body to generate a propagating wave, and transform frictions from ground into push forces for moving. (2) Concertina: This locomotion mode is employed when a snake is in narrow spaces. Snakes contract and extend their body to move, just like a concertina. (3) Side-winding: Snakes usually perform side-winding locomotion in desert. They lift a lot of parts of their body and just put some parts on the ground as fulcrums to move in the lateral direction of their body. (4) Rectilinear: It is a locomotion mode for boa constrictor. Through interaction of their muscles and ribs, snakes move their giant body as a straight line.

To mimic different kinds of postures of a real snake, snake robots are always designed to be modular with a high degrees of freedom and homogeneity. We classify the general unit modules of snake robots to four classes: (a) Non-wheeled: There is no wheel equipped on the modules (Kotay and Rus, 2000; Li et al., 2004; Ma, 2004; Saito et al., 2002); (b) Wheeled: Wheels are equipped on the modules (Crespi et al., 2005; Kimura and Hirose, 2002; Mori and Hirose, 2001); (c) Expandable and contractible: The joint between two modules is not active, but rotated by expanding and contracting of the link that equipped on both sides of the module (Aoki et al., 2002); (d) Reconfigurable: The modules are multi-functions. They can be not only configured to a snake robot, but also other three-dimensional structure (Castano et al., 2002; Kurokawa et al., 2005).

2. MODULAR DESIGN

Synthesizing the design ideas of the above mentioned snake robots, we know that snake robots are usually configured by a lot of homogeneous modular units. The units are designed to have following key features.

1. Homogeneity: All of the unit modules have the same structures and functions, and their roles can be replaced by each other. This feature lets a modular robot have higher mechanical failure robustness and reconfiguring capability.

2. High degrees of freedom: One unit module or two assembled unit modules have at least one degree of freedom in motion, including pitch, yaw and roll, or expanding and contracting.

3. High capability of connection: One unit module has at least one independent connector and can connect with the other unit modules. With this feature, the unit modules can be assembled to become a 2-D or 3-D structure.

4. Self power supply: One unit module has its own power supply system. With this feature, there is no limit caused by lines for power supply or signal transmission.

5. Sensing capability: One unit module has at least one sensor and can obtain its own states and information from environment.

6. Communication capability: One unit module can communicate with others. With this feature, the unit module can obtain the information from the others and send commands back to them.

7. Computational capability: Each unit module has its own central processing unit. With its own states and information from environment, it can compute through a predefined algorithm and decide the optimal motion strategy.

Considering the above mentioned features, three kinds of basic unit modules of snake robots are designed, including non-wheeled and wheeled ones. Then the software, Working Model 3D, is used to construct these modules and simulate related motion performance.

2.1 Non-Wheeled Arms Modules

Figure 1(a) shows a unit module. It is formed with two cubes and two arms. The two blue arms are fixed on the both sides of the gray cube, respectively, and there is a roll joint between the gray cube and the purple cube, as shown in Figure 1(b). The unit module can be connected to another by the two arms, and there is a pitch joint between two assembled unit modules, as shown in Figure 1(c). If two unit modules are assembled vertically as a "bi-module", then the "bi-module" has two degrees of freedom, pitch and yaw, as shown in Figure 1(d). With the two degrees of freedom, the snake robot can achieve three-dimensional postures.

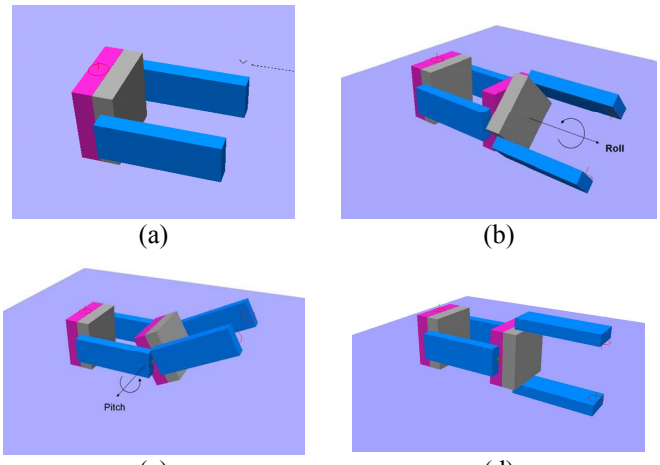

(a) (b) (c) (d)

Figure 1. (a) Non-wheeled arms module. (b) Two assembled non-wheeled arms modules. There is a roll joint between the purple cube and the gray one. (c) Two assembled non-wheeled arms modules. There is a pitch joint between the two arms and the purple cube. (d) The "bi-module" is configured by two assembled vertically non-wheel cube modules. There are two degrees of fredom, pitch and yaw.

2.2 Non-Wheeled Cube Modules

Considering the non-wheeled arms modules, several problems are found. (1) The unit modules are easy to tumble because the two arms are connected to the outer sides of the cube. (2) Two unit modules are hard to connect precisely and synchronously because there are two connectors between the arms of the first module and the cube of the other one. (3) The arms of a unit module could affect roll motion of the neighboring module. To improve these problems, a new kind of unit module is designed.

Figure 2(a) shows the new unit module. There is one yaw joint between the black cube and the white one. And there is also a roll joint between two assembled unit modules, as shown in Figure 2(b). If two unit modules are assembled vertically as a "bi-module", then the "bi-module" has two degrees of freedom, pitch and yaw, as shown in Figure 2(c). With the two rotational degrees of freedom, the snake robot can achieve three-dimensional postures.

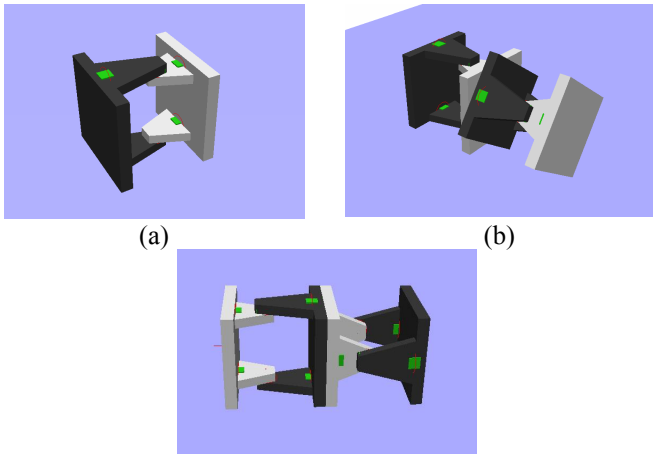

(a) (b) (c)

Figure 2. (a) Non-wheeled cube module. (b) Two assembled non-wheeled cube modules. There is a roll joint between the two modules. (c) The "bi-module" is formed with two assembled vertically non-wheel cube modules. There are two degrees of freedom, pitch and yaw.

2.3 Wheeled Modules

Different from the two above mentioned non-wheeled modules, another kind of unit module with wheels is designed, as shown in Figure 3(a). Two wheels are equipped on both sides of the unit car. One unit car does not have its own rotational degree of freedom, but there is one yaw joint between two assembled unit cars, as shown in Figure 3(b).

In fact, the wheeled modules have no degrees of freedom of roll and less adaptability to terrain, but the wheels provide an important condition for snake locomotion, that is directional friction. And that is why lots of snake robots are wheeled.

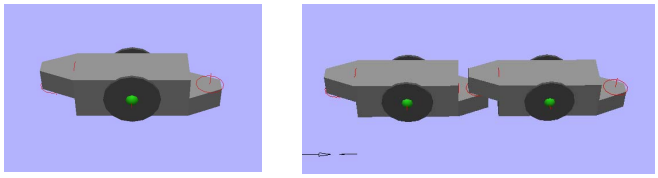

(a) (b)

Figure 3. (a)Wheeled module. There are two wheels equipped on both sides of the unit module. (b) Two assembled unit cars. There is a yaw joint between them.

3. SIMULATION RESULTS

To apply the theory of snake locomotion (Gray, 1946; Hirose, 1993; Saito et al., 2002) to the design of unit modules, several simulations of three kinds of unit modules are performed using the software, Working Model 3D. The simulation results are discussed as follows.

3.1 Non-Wheeled Arms Modules

In this simulation, twenty non-wheeled arms unit modules are assembled vertically to be a snake robot, as shown in Figure 4, which has two kinds of degrees of freedom, pitch and yaw. The weight of one unit module is 6.4 kg, and the length is 35.5 cm.

The snake robot is put on a planar ground with friction. Each yaw joint is set to swing as a sinusoidal wave and there is a phase delay of 36° between two assembled unit modules, in other words, waves propagate from the head to the tail of the snake robot body. This kind curve of the snake robot body is well known as Serpenoid curve, proposed by Hirose (Hirose, 1993), and this curve is close to the curve of Serpentine locomotion of real snake. However, the snake robot cannot move forward, it just slides at the original location.

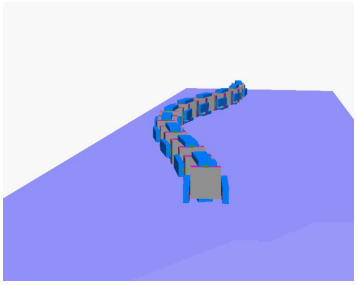

Figure 4. Twenty non-wheeled arms unit modules are assembled vertically to be a snake robot. Each yaw joint is set to swing as a sinusoidal wave and there is a phase delay of 36° between two assembled unit modules.

Considering the theory of snake locomotion proposed in (Gray, 1946), the driving force of Serpenoid locomotion is formed by the lateral force from rugged ground. To simulate the rugged ground, twenty one free pegs are put on both sides of the snake robot, as shown in Figure 5(a). Hence, when the snake robot acts as a Serpenoid curve and pushes the pegs, the pegs generate resistances back to the snake robot, and these resistances form a forward driving force to push the snake robot to move forward, as shown in Figure 5(b). This simulation result shows that the serpentine locomotion can transform side resistances into the forward driving forces.

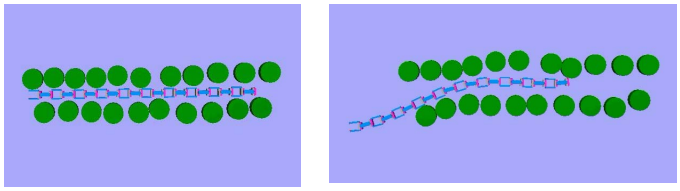

(a) (b)

Figure 5. (a) To perform the continuous side resistance from environment, 21 free pegs are put at the both sides of the snake robot. (b) Resistances form a forward driving force to push the snake robot to move forward.

3.2 Non-Wheeled Cube Modules

In the following simulations, twenty four non-wheeled cube modules are assembled in the same direction to be a snake robot which has twenty four yaw joints. The weight of one unit modules is 0.646 kg, and the length is 21 cm. Simulations with different joint rotations and conditions of ground are listed in Table 1 and performed as follows.

In the first simulation, as Figure 6 shows, the snake robot is put on a planar ground. Each yaw joint of the snake robot is set to swing as a sinusoidal wave and the amplitude of the sinusoidal wave is 45°. There is a phase delay of 30° between two assembled unit modules. The coefficient of friction between the snake robot and the ground is 50 and the coefficient of resilience is 0. In this simulation, the snake robot serpentine on the ground but cannot move forward effectively. That is, it just swings and slips at the original location. After two periods of the joints swing, the displacement of the snake robot head in x-direction is 14 cm.

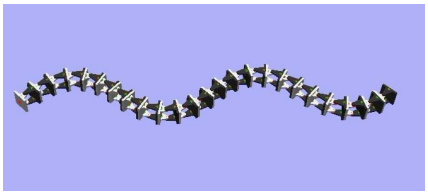

Figure 6. Twenty four non-wheeled cube modules are assembled in the same direction to be a snake robot. The yaw joints rotate as a sinusoidal wave with amplitude of 45° and there is phase delay of 30° between two assembled unit modules.

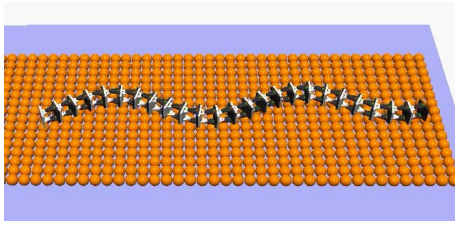

Figure 7. To perform effect from rugged ground, the fixed balls are put between the snake robot and ground.

Furthermore, to perform effects from rugged ground, fixed balls are put between the snake robot and ground, as shown in Figure 7, and the radius of the fixed balls is 7 cm. In the second simulation, the yaw joints of the snake robot swing as a sinusoidal wave with amplitude of 45°, and there is a phase delay of 30° between two assembled unit modules. The coefficient of friction between the fixed balls and the snake robot is 50 and the coefficient of resilience is 0. Observing the simulation result, the snake robot still cannot move and the displacement in x-direction is -7.5 cm after two periods of the sinusoidal wave. In the third simulation, the coefficient of friction is cancelled. Observing the result, after two periods of the sinusoidal wave, the displacement of the snake robot head in x-direction is 32.5 cm, the moving of the snake robot is more effective than the above two cases. In the fourth simulation, the coefficient of friction is 0, but the coefficient of resilience is set to be 0.5. Observing the simulation result, after two periods of the yaw joints swing, the displacement of the snake robot head in x-direction is 23.5 cm. We can find that the isotropic friction cancel the driving force for the forward motion of the snake robot and let it slide, and there is

no obviously affect whether resilience exist or not. When the snake robot serpentine, the collision between the snake robot and the fixed balls provide the forward driving force and the snake robot can move forward effectively.

In the fifth to eighth simulations, the amplitude of the sinusoidal wave which the yaw joints swing is changed to 30°, 60°, 75° and 90°, respectively. Observing the simulation results, after two periods of the sinusoidal wave, the displacements of the snake robot head are 41cm, -63.5cm, -55.5cm and -10cm, respectively. We can find that when the amplitude decreases from 45° to 30°, the serpentine of the snake robot become more effective. However, when the amplitude increases from 45° to 60°, the snake robot starts to slide and move backward.

In the ninth to thirteenth simulations, the radius of the fixed balls are increased to 12 cm, and the amplitude of the sinusoidal wave which the yaw joints swing is 30°, 45°, 60°, 75° and 90°, respectively. Observing the simulation results, after two periods of the sinusoidal wave, the displacements of the snake robot head are 14.5, -16.5, -25, -34 and -19.5. When the amplitude increase from 30° to 45°, the snake robot starts to slide and moves backward.

From the above simulation results, we find that the less amplitude of the sinusoidal wave, the more moving speed of the snake robot, and when the radius of the fixed balls increase, the yaw joints of the snake robot need to swing with less amplitude to achieve the same moving speed.

Then, to perform three dimensional postures, the snake robot is reconfigured. The twenty four non-wheeled cube modules are assembled vertically to have two kinds of joints, pitch and yaw, and totally twelve pitch joints and twelve yaw joints. The conditions and results of the following simulations are listed in Table 2 and discussed as follows.

In the fourteenth simulation, to perform the side-winding locomotion, twelve yaw joints are set to swing as a sinusoidal wave with amplitude of 30°, and there is a phase delay of 30° between two neighbor yaw joints. The other twelve pitch joints are set to swing as a sinusoidal wave with amplitude of 10° and there is a phase lead of 60° between two neighbor pitch joint, then the part of wave crest of the snake robot body are lifted, as shown in Figure 8, just like the side-winding locomotion of real snake. The snake robot is put on a planar ground with coefficient of friction of 100 and performs the side-winding locomotion. Observing the simulation result, after two periods of the sinusoidal wave which the yaw joints swing, the displacement in x-direction of the snake robot head is 58 cm and the displacement in y-direction is 1 cm.

In the fifteenth to nineteenth simulations, the condition of the ground is the same, and the amplitude of sinusoidal wave which the yaw joints swing increases from 30° to 45°, 60°, 75°, 90° and 120°, respectively. Observing the simulation results, the displacements in x-direction after two periods of the sinusoidal wave are 168 cm, 265 cm, 425 cm, 485 cm and 550 cm, respectively. The displacements in y-direction after two periods of the sinusoidal wave also increase to 51 cm, 190 cm, 305 cm, 420 cm and 330 cm, respectively.

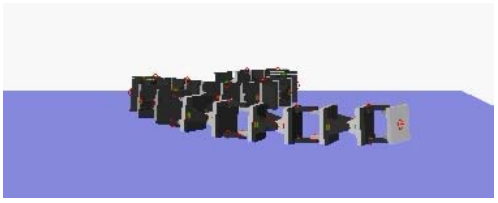

Figure 8. Twenty four non-wheeled cube modules are assembled vertically to be a snake robot with twelve yaw joints and twelve pitch ones. The parts of wave crest of the snake robot body are lifted.

According to the simulation results, we find that, when the amplitude of sinusoidal wave increases, the moving speed of the snake robot increases and the angle of moving direction of the snake robot also increases.

In the twentieth simulation, to mimic the Concertina locomotion of real snakes, the degrees of the yaw joints are set to be 0, and the pitch joints swing as a sinusoidal wave with amplitude of 30°, and there is a phase lead of 30° between two neighbor pitch joints. In other words, the wave propagate vertically from the tail of the snake robot to the head. And the snake robot is put on a planar ground with coefficient of friction of 100. Observing the simulation result, the snake robot move forward effectively and the displacement of the snake robot head in x-direction is 98 cm after two periods of the sinusoidal wave the pitch joints swing.

Furthermore, in the twenty-first to twenty-third simulations, the conditions of environment is the same and the amplitude of the sinusoidal wave which the pitch joints swing increases to 60°, 90° and 120°, respectively. Observing the simulation results, the displacements of the snake robot head in x-direction is 206 cm, 283 cm and 350 cm. We find that the more amplitude of the sinusoidal wave, the more moving speed of Concertina locomotion of the snake robot.

3.3 Wheeled Modules

In the following simulations, the wheeled modules are assembled to be a snake robot, the weight of one module is 0.094 kg and the length is 28 cm. To fit Serpenoid curve derived in (Saito et al., 2002), each yaw joint between two neighbor modules are set to swing a sinusoidal wave. The yaw joint angles are computed by (1). In (1), the $\varphi_i(t)$ is the i-th joint angle at time t, the parameter n denotes the number of assembled modules, a is involved in sinusoidal wave amplitudes the yaw joints swing, b is involved in the number of the wave of Serpenoid curve, and c is involved in the curvature of Serpenoid curve. The parameters a, b and c can be tuned for different postures.

$$\begin{aligned} &\phi_i(t) = \alpha \sin(\omega t + (i-1)\beta) + \gamma, \quad (i = 1,\ldots,n-1) \\ &\alpha = a\left|\sin(\frac{\beta}{2})\right|, \quad \beta = \frac{b}{n}, \quad \gamma = -\frac{c}{n} \end{aligned} \tag{1}$$

In the twenty-fourth simulation, two wheeled modules are assembled to be a snake robot with one yaw joint and the yaw

joint is set to rotate as the $\varphi_i(t)$, where n is 2, and a, b and c are set to be 78.5°, 360° and 0°, respectively. And the snake robot is put on a planar ground with coefficient of friction of 50. Observing the simulation results, the snake robot just slides and oscillates at the original location. The displacement of the snake robot head in x-direction is 1.5 cm after two periods of the sinusoidal wave.

In the twenty-fifth simulation, three wheeled modules are assembled to be a snake robot and the parameters of Serpenoid curve and the condition of the ground is the same. Observing the simulation result, the snake robot also slides and oscillates but moves a little distance. The displacement of the snake robot head in x-direction is 5.5 cm after two periods of the sinusoidal wave.

In the twenty-sixth simulation, the number of assembled wheeled modules is increased to 4, as shown in Figure 9, and the parameters of Serpenoid curve and the conditions of the ground are the same. Observing the simulation result, the snake move forward effectively with a constant speed. Figure10 shows the position of the snake robot head versus time and the purple line represents the position in x direction, red one represents the position in y-direction, green one represents the position in z-direction. The displacement of the snake robot head in x-direction is 43.5 cm after two periods of the sinusoidal wave.

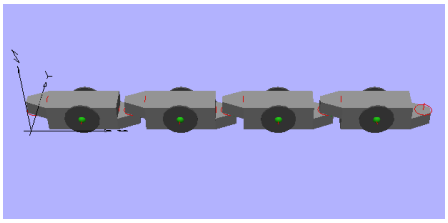

Figure 9. Four unit cars are assembled to form a snake robot.

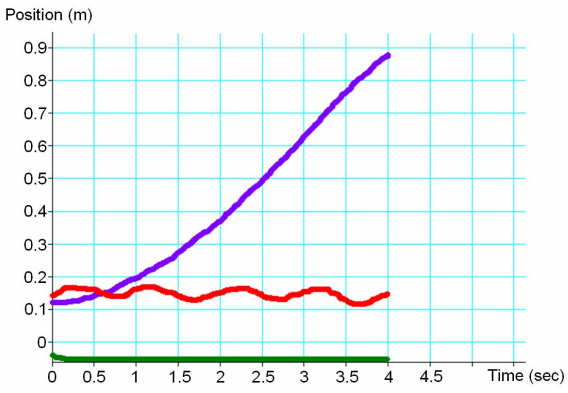

Figure 10. The diagram that the position of the snake robot head versus time and the purple line represents position in x-direction, red one represents the position in y-direction, green one represents the position in z-direction.

In the twenty-seventh and the twenty-eighth simulations, the number of the assembled wheeled modules is increased to 5 and 6, respectively. The parameters of Serpenoid and the condition of the ground are the same. Observing the simulation results, the snake robot can also move forward effectively and stably. After two periods of the sinusoidal wave, the displacements of the snake robot head in x–direction is 30 cm and 65 cm, respectively.

According to the above simulation results, we believe that when number of the wave of Serpenoid curve is the same, there exists a limit value, and if the number of assembled wheeled modules is more than this limit value, the snake robot can achieve a constant speed in steady state. Under the conditions in the above simulations, this limit value is 4.

In the twenty-ninth simulation, the parameter ω is decreased to π and the parameters of Serpenoid curve are the same as those in the twenty-sixth simulation. Then the displacement of the snake robot head in x-direction after two periods is 39.5. In the thirtieth simulation, the parameter ω is increased to 4π and the parameters of Serpenoid curve are the same as those in the twenty-sixth simulation. Observing the simulation result, the snake robot just slide at the original location and does not move forward. It means that, when angular speed of yaw joints is too larger, the snake robot starts to slide. In the thirty-first simulation, the coefficient of friction is increased to twenty times of the one in the thirtieth simulation, and the parameters of Serpenoid are the same. Observing the simulation result, the forward moving of the snake robot is more effective than the snake robot in the thirtieth simulation. And the displacement of the snake robot head in x-direction after two periods of the sinusoidal wave is 28.6 cm. This simulation result means that the larger friction actually can stabilize the sliding of the snake robot. In the last simulation, parameter a is double of the one in the twenty-sixth simulation. The other parameters of Serpenoid and the conditions of the ground are the same. Observing the simulation results, we find that the snake robot slide lightly, but still keep moving forward and the displacement of the snake robot head in x-direction after two periods of the sinusoidal wave is 32.5 cm. We believe that the sliding of the snake robot is also caused by the increasing of angular speeds of the yaw joints.

4. CONCLUSIONS AND FUTURE WORKS

In this study, three different kinds of unit modules are designed, including non-wheeled arms modules, non-wheeled cube modules and wheeled modules. By using the software, Working Model 3D, these three kinds of unit modules are assembled to be three snake robots. Related simulations with different snake locomotion modes and environment conditions are performed. According to the simulation results, the effect to the motion of the snake robot which is caused by different configuration of the unit modules, parameter of locomotion modes, and conditions of environment can be understood. In the future, the hardware design of the unit modules will be realized and used to assemble to snake robots. Furthermore, the mathematical modeling, dynamical analysis, and design of control system will be further investigated.

ACKNOWLEDGEMENTS

The authors would like to thank the anonymous referees for their constructive comments and suggestions. This work was supported in part by the National Science Council, Taiwan, ROC, under the grants: NSC 95-2221-E-002-303-MY3, NSC 96-2218-E-002-030, and DOIT/TDPA: 95-EC-17-A-04-S1-054.

REFERENCES

Aoki, T., H. Ohno and S. Hirose (2001). Design of Slim Slime Robot II (SSR-II) with Bridle Bellows. In *Proceedings of IEEE International Conference on Intelligent Robots and Systems*, Lausanne, Switzerland, pp. 835-840.

Castano, A., A. Behar and P.M. Will (2002). The Conro Modules for Reconfigurable Robots. *IEEE/ASME Transactions on Mechatronics*, Vol. 7, No. 4, pp. 403-409.

Crespi, A., A. Badertscher, A. Guiganrd and A.J. Ijspeert (2005). Swimming and Crawling with an Amphibious Snake Robot. In *Proceedings of_IEEE International Conference on Robotics and Automation*, Barcelona, Spain , pp. 3035-3039.

Gray, J. (1946). The Mechanism of Locomotion in Snakes. *Journal of Experimental Biology*, Vol. 23, No. 2, pp. 101-120.

Hirose, S. (1993). Biologically Inspired Robots. *Oxford University Press*.

Kimura, H. and S. Hirose (2002). Development of Genbu: Active Wheel Passive Joint Articulated Mobile Robot. In *Proceedings of IEEE International Conference on Intelligent Robots and Systems*, Lausanne, Switzerland, pp. 823-828.

Kotay, K. and D. Rus (2000). The Inchworm Robot: A Multi-Functional System. *Autonomous Robots*, Vol. 8, No. 1, pp. 53-69.

Kurokawa, H., K. Tomita and S. Kokaji (2005). Distributed Self-reconfiguration Control of Modular Robot M-TRAN. In *International Conference on Mechatronics & Automation*, Niagara Falls, Canada, pp. 254-259.

Li, B., L. Chen and Y. Lv (2004). Development of a Snake-Like Robot Adapting to the Ground, *International Conference on Control, Automation, Robotics and Vision*, Kunming, China, pp. 273-277.

Ma, S. (2004). A Serpentine Robot Based on 3 DOF Coupled-driven Joint. In *Proceedings of the 2004 IEEE International Conference on Robotics and Biomimetics*, Shenyang, China, pp. 70-75.

Mori, M. and S. Hirose (2001). Development of Active Cord Mechanism ACM-R3 with Agile 3D Mobility. In *Proceedings of IEEE International Conference on Intelligent Robots and Systems*, Maui, HI , pp.1552-1557.

Saito, M., M. Fukaya and T. Iwasaki (2002). Serpentine Locomotion with Robotic Snakes. *IEEE Control Systems Magazine*, Vol. 22, pp. 64-81.

Table 1. The simulation parameters of the snake robot that is formed by non-wheeled cube modules.

	Mode	No. of wave	Amp. of yaw	Fric.	Res	Environment fixed balls	x-disp. in 2 periods	y-disp in 2 periods
1	Serpentine	1	45	50	0		14	-80
2	Serpentine	1	45	50	0	(r=0.07)	-7.5	-43
3	Serpentine	1	45	0	0	(r=0.07)	32.5	-1.5
4	Serpentine	1	45	0	0.5	(r=0.07)	23.5	2.5
5	Serpentine	1	30	0	0.5	(r=0.07)	41	8
6	Serpentine	1	60	0	0.5	(r=0.07)	-63.5	-29
7	Serpentine	1	75	0	0.5	(r=0.07)	-55.5	-7
8	Serpentine	1	90	0	0.5	(r=0.07)	-10	28
9	Serpentine	1	30	0	0.5	(r=0.12)	14.5	-29
10	Serpentine	1	45	0	0.5	(r=0.12)	-16.5	-23
11	Serpentine	1	60	0	0.5	(r=0.12)	-25	10
12	Serpentine	1	75	0	0.5	(r=0.12)	-34	-4.5
13	Serpentine	1	90	0	0.5	(r=0.12)	-19.5	39

Table 2. The simulation parameters of the snake robot that is formed by non-wheeled cube modules.

No	Mode	No. of wave	Amp. Of yaw	Amp. Of pitch	Fric.	Res	x-disp. in 2 periods	y-disp in 2 periods
14	Sidewinding	1	30	10	100	0	58	1
15	Sidewinding	1	45	10	100	0	168	51
16	Sidewinding	1	60	10	100	0	265	190
17	Sidewinding	1	75	10	100	0	425	305
18	Sidewinding	1	90	10	100	0	485	420
19	Sidewinding	1	120	10	100	0	550	330
20	Concertina	1	30	0	100	0	98	0
21	Concertina	1	60	0	100	0	206	0
22	Concertina	1	90	0	100	0	283	0
23	Concertina	1	120	0	100	0	350	0

Table 3. The simulation parameters of the snake robot that is formed by wheeled modules.

No.	n	a	b	c	ω	Fric.	x-disp in 2 periods	y-disp in 2 periods
24	2	78.5	360	0	2π	50	1.5	-0.5
25	3	78.5	360	0	2π	50	5.5	1
26	4	78.5	360	0	2π	50	43.5	1
27	5	78.5	360	0	2π	50	30	11.5
28	6	78.5	360	0	2π	50	65	8
29	4	78.5	360	0	π	50	39.5	-6.5
30	4	78.5	360	0	4π	50	-0.65	-12
31	4	78.5	360	0	4π	1000	28.6	0.5
32	4	157	360	0	2π	50	32.5	8